Oxetane modified antisense oligonucleotides promote RNase H cleavage of the complementary RNA strand in the hybrid duplex as efficiently as the native, and offer improved endonuclease resistance

Pushpangadan I. Pradeepkumar and Jyoti Chattopadhyaya *

Department of Bioorganic Chemistry, Box 581, Biomedical Center, University of Uppsala, S-751 23 Uppsala, Sweden. E-mail: jyoti@bioorgchem.uu.se; Fax: +4618554495; Tel: +4618471577

Received (in Cambridge, UK) 16th July 2001, Accepted 17th August 2001
First published as an Advance Article on the web 25th September 2001

Although the T_m drops ~6 °C/modification (note: T_m loss is ~10 °C/mismatch) in the oxetane, [1-(1′,3′-*O*-anhydro-β-D-psicofuranosyl)thymine, **T**], modified antisense (AON)–RNA heteroduplexes, the relative rates of the complementary RNA cleavage by RNase H remain the same as or comparable to that of the native counterpart. The RNA cleavage in the native hybrid duplex was 68 ± 3% (T_m = 44 °C), whereas it was found to be 64 ± 10% for the single **T** modified AON–RNA duplex (T_m = 39 °C), 56 ± 9% for the double **T** modified AON–RNA duplex (T_m = 33 °C) and 60 ± 7% for the triple **T** modified AON–RNAs (T_m = 26 °C). The oxetane modifications in AON reduce the endonuclease cleavage (DNase 1) significantly. One modification gives ~2-fold protection and three modifications give ~4-fold protection compared to that of the native. Introductions of both interior oxetane modifications in conjunction with the 3′-DPPZ (dipyridophenazine) group give the resulting AON–RNA hybrid an RNase H cleavage rate at least the same as that of the native counterpart, which, additionally, gives full stability against both exo- and endonucleases. The conformational transmission of the constrained 3′-*endo* sugar of the oxetane nucleotide in the AON strand is found to be transmitted up to a stretch of five nucleotides in the heteroduplex as is evident by the RNase H resistance to the cleavage of the complementary RNA strand, thereby showing that this five-nucleotide region most probably takes up a local RNA–RNA type conformation. This is the *first report* of an antisense oligonucleotide construct which fulfils three important criteria simultaneously: (1) the modified AON promotes the complementary RNA cleavage by RNase H at an efficiency comparable to that of the native counterpart, (2) the modified AON has substantially more endonuclease stability than that of the native AON, and finally, (3) the DPPZ group at the 3′-end provides the expected exonuclease stability. This also shows that the T_m increase of the AON–RNA hybrid duplex is not mandatory for RNase H promoted destruction of the target RNA.

Introduction

In pursuit of potential antisense drugs, much effort has been devoted in recent times to the synthesis of antisense oligonucleotides (AONs) having sugar modified nucleosides.[1] Among these, the AONs containing conformationally constrained nucleosides[2] have received much attention because of the fact that upon incorporation of the conformationally constrained 3′-*endo* (North) nucleosides into the AON, the corresponding hybrid AON–RNA duplex is driven to the RNA–RNA type conformation with a higher thermodynamic stability, which allows the AON to block the target RNA function effectively.[3] The RNA moiety of these AON–RNA hybrids was however found to be insensitive towards RNase H promoted cleavage, which is identified as one of the important pathways to deliver antisense action.[4] To address the issue, chimeric AONs have been synthesized, which provide a natural AON–RNA region in the hybrid duplex for the recognition and cleavage by RNase H.[5] But all these efforts were overshadowed by the slower hydrolysis of the AON–RNA hybrids by RNase H compared to their native counterparts,[6] except for some methylphosphonate chimeras.[7] Recently, we have demonstrated[8] that introduction of a single North-constrained nucleoside, [1-(1′,3′-*O*-anhydro-β-D-psicofuranosyl)thymine] (**T**) (Fig. 1), into an AON does not alter the global helical structure of the corresponding AON–RNA hybrid as compared to the native counterpart. Despite the fact that a series of single **T** modified AON–RNA hybrid duplexes showed a drop of ~6 °C/modification in T_m, they were however cleaved by RNase H with an efficiency comparable to that of the native counterpart.[8] We also found that the target RNA strand in the hybrid AON–RNA duplex was resistant up to five nucleotides towards the 3′-end[8] from the site opposite to **T** introduction in the AON strand.

We now report that the incorporation of up to three **T** residues in the modified AONs, irrespective of their positions in the AON chain, shows the 5-nucleotide resistance region in the RNA strand from the site opposite to **T** in the corresponding AON–RNA hybrid to RNase H. Despite the fact that these **T** modified AON–RNA duplexes were destabilized by 6 to 18 °C (~6 °C/modification, and the corresponding loss in net free energy ($\Delta\Delta G^\circ_{298}$) ≈ 9 kJ mol^{-1}) compared to the native counterpart, they were found to be as good a substrate for RNase H as the native hybrid duplex. The exact number of **T** modifications in the AON was found to play an important role in exhibiting resistance towards endonucleotic degradation, although they did not have any effect against the 3′-exonuclease activity. It was also found that the thermodynamic stability was partially restored by the introduction of the dipyridophenazine (DPPZ) moiety at the 3′-end of these **T** modified AONs, which also gave enhanced protection towards 3′-exonucleases. We thus demonstrate that the AON containing multiple **T**s in combination with the 3′-DPPZ group is a unique entrant into the family of

 DOI: 10.1039/b106281f

Native	**AON (1)**:	3′-d(CTTCTTTTTTACTTC)-5′
Single **T** modified	**AON (2)**:	3′-d(CT**T**CTTTTTTACTTC)-5′
	AON (3):	3′-d(CTTCT**T**TTTTACTTC)-5′
	AON (4):	3′-d(CTTCTTTT**T**TTACTTC)-5′
	AON (5):	3′-d(CTTCTTTTTT**T**ACTTC)-5′
Double **T** modified	**AON (6)**:	3′-d(CT**T**CTT**T**TTTACTTC)-5′
	AON (7):	3′-d(CT**T**CTTTT**T**TTACTTC)-5′
	AON (8):	3′-d(CT**T**CTTTTT**T**TACTTC)-5′
	AON (9):	3′-d(CT**T**CTTTTTT**T**ACTTC)-5′
Triple **T** modified	**AON (10)**:	3′-d(CT**T**C**TT**TTTTACTTC)-5′
	AON (11):	3′-d(CT**T**CTT**T**TTTAC**T**TC)-5′
	AON (12):	3′-d(CT**T**CTTTT**T**TTAC**T**TC)-5′
	AON (13):	3′-d(CT**T**CTTTTT**T**TAC**T**TC)-5′
	AON (14):	3′-d(CT**T**CTTTTTT**T**AC**T**TC)-5′
All **T** modified	**AON (15)**:	3′-d(C**TT**C**TTTTTT**AC**TT**C)-5′
Single mismatched	**AON (16)**:	3′-d(CTTCT**G**TTTTACTTC)-5′
	AON (17):	3′-d(CTTCT**A**TTTTACTTC)-5′
	AON (18):	3′-d(CTTCT**C**TTTTACTTC)-5′
Triple mismatched	**AON (19)**:	3′-d(CTACAATTTTACTTC)-5′
	AON (20):	3′-d(CTACTTATTTACATC)-5′
	AON (21):	3′-d(CTACTTTATTACATC)-5′
	AON (22):	3′-d(CTACTTTTATACATC)-5′
	AON (23):	3′-d(CTACTTTTTAACATC)-5′
Native **DPPZ**	**AON (24)**:	**DPPZ**3′-d(CTTCTTTTTTACTTC)-5′
3**T** mod.with **DPPZ**	**AON (25)**:	**DPPZ**3′-d(CT**T**CTTT**T**TTAC**T**TC)-5′
Target	**RNA (26)**:	5′-r(GAAGAAAAAAUGAAG)-3′

T =

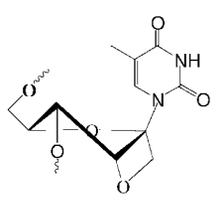

DPPZ =

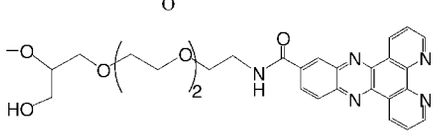

Fig. 1 Sequences of various AONs and their target RNA.

potential antisense drugs. We also show that the minimal introduction of **T** residues into the AON strand can be effectively used as a tool to produce desired RNA fragments by engineering the RNase H cleavage site in the AON–RNA duplex, which, we believe, should have considerable applications in the field of RNA engineering.

Results and discussion

All of the **T** modified AON–RNA duplexes, except the one in which all of the Ts were replaced by **T**s (as in AON (**15**), Fig. 1), were found to be substrates for RNase H. Since all of the **T** modified AONs (**2**)–(**14**) (Fig. 1) showed lower binding affinity towards the RNA target (as revealed by T_m and the $\Delta G°_{298}$ of the corresponding AON–RNA hybrid, Table 1), it was important to check whether this effect is due to the loss of hydrogen bonding between **T** in the AON and the complementary A in the target RNA sequence. We have therefore introduced mismatches [as in AONs (**16**)–(**23**), Fig. 1] at the site of **T** modifications [as in AONs (**2**)–(**14**), Fig. 1] and compared their properties. The following observations give an insight into the behavior of various **T** modified AON–RNA hybrids towards RNase H cleavage as well as their stability toward endo- and exonucleases.

(1) The experiments determining the extent of RNA cleavage in these hybrid duplexes by *E. coli* RNase H1 have been performed under uniform conditions. They were repeated at least four times using 1 : 1 AON–RNA duplex and 0.3 unit of RNase H at 21 °C (see Experimental section), and the average values of these experiments (after 2 h of incubation) are reported here (Figs. 2–7 for PAGE pictures and Table 2 for percentage of RNA cleavage). The RNA in the native hybrid [AON (**1**)–RNA (**26**)] was hydrolyzed to 68 ± 3%. The target RNA with all of the single **T** modified AONs (**2**)–(**5**) was hydrolyzed to 64 ± 10% (Fig. 2); with double **T** modified AONs (**6**)–(**9**) the target RNA was hydrolyzed to 56 ± 9% (Fig. 3); with triple **T** modified AONs (**10**)–(**14**) the target RNA was hydrolyzed to 60 ± 7% (Fig. 5) and finally the 5-nucleotide resistance rule[8] of the complementary RNA strand against RNase H, found for the single **T** modified AONs, was valid for both the double and triple **T** modified AONs.

(2) In the AONs (**16**)–(**18**)–RNA (**26**) hybrid duplexes with a single mismatch [introduced at the same position as the **T** in AON (**3**)], the RNA was cleaved at a rate comparable to that of the native counterpart although a 10 °C loss of T_m ($\Delta\Delta G°_{298}$ ≈ 14–18 kJ mol^{-1}, Table 1) was recorded owing to the mismatch. They also showed additional cleavage sites at A9 and A8 (Fig. 4), which were absent in the AON (**3**)–RNA (**26**) duplex cleavage pattern. These two observations therefore show that the recognition of **T** *vis-à-vis* a mismatch in the AON strand by the target RNA is indeed different, most probably owing to the fact that **T** was perhaps partially hydrogen bonded (see below for our observations on triple **T** modified AONs (**10**)–(**14**) and the corresponding triple mismatched AONs (**19**)–(**23**) for comparison).

(3) The five-nucleotide resistance rule[8] to the RNase H cleavage of the RNA in the AON–RNA hybrids in all of the single **T**, double **T** and triple **T** modified AONs (**2**)–(**14**) allowed us to engineer a *single cleavage site* for RNase H in the target RNA, as exemplified in the AON (**13**)–RNA (**26**) hybrid duplex (Fig. 5). The single RNA cleavage site was earlier shown to occur in the case of 2′-*O*-methyl modified chimeric AON–RNA duplex[9] in which all the central 2′-deoxynucleotides except the middle nucleotide have been shown to adopt an RNA-type conformation by NMR spectroscopy.[10] Since the CD spectra showed that all of our **T** modified AONs (**2**)–(**14**)–RNA (**26**) hybrid duplexes have a global structure that corresponds to a DNA–RNA type duplex (indicating that our AONs retain the B-DNA type helical conformation in the hybrid, see Figs. 8–10), we conclude that the 5-nucleotide resistance rule observed with our **T** modified AONs is owing to more subtle local microscopic conformational (and/or hydration) change, which is only detectable by the enzyme, not by the CD. This seems to indicate that the conformational changes of the sugar–phosphate backbone on average, induced by the N-sugar constraining the **T**-residues in the modified AONs, do not affect the base stacking in the **T**-modified AON–RNA hybrids in a significant manner. Most probably the RNase H detected conformational change, which has been found to span up to 5 nucleotides owing to the introduction of a single North-constrained nucleotide in the AON strand, is restricted only to the sugar–phosphate moieties, and this does not alter the base stacking and helicity of the hybrid duplex. This might suggest that there is no sugar–phosphate induced co-operative effect on the conformation of the stacked helices, *i.e.* the sugar pucker change is uncoupled from the base-stacking. This may explain why the CD is unable to detect the conformational changes orchestrated by the sugar modification, since the CD only reflects the base stacking geometry.

(4) When the Ts in the triple **T** modified AONs were replaced by A, as in mismatched AONs (**19**)–(**23**)–RNA (**26**) duplex, no target RNA hydrolysis by RNase H was observed except with that of mismatched AON (**19**) (Fig. 6). In AON (**19**), the mismatches are close to each other towards the 3′-end, providing a continuous stretch of 8 matched basepairs at the 5′-end. Thus the the target RNA in the AON (**19**)–RNA (**26**) hybrid is cleaved at a half-rate (35 ± 2%) compared to that of the native hybrid (68 ± 3%) or the corresponding three **T** modified AON

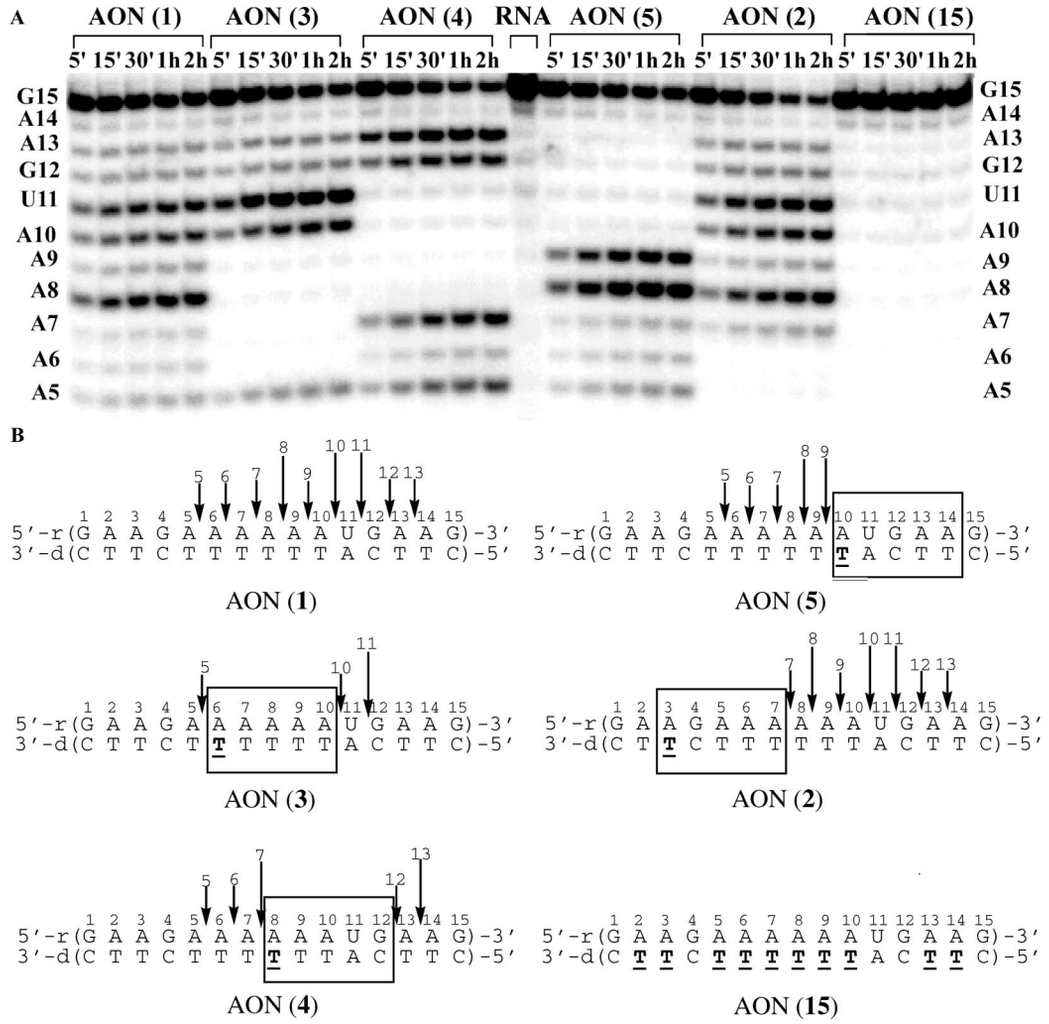

Fig. 2 (**A**) The PAGE analysis of RNase H hydrolysis of the hybrid duplexes, AON (**1**)–(**5**) and AON (**15**)–RNA (**26**). Time after the addition of the enzyme is shown on the top of each gel lane. The length and sequence of 5′-^{32}P-labeled RNAs formed upon enzymatic cleavage are shown on the left and right side of the gel and they were deduced by comparing the migration of products with those oligonucleotides generated by partial digestion of the target RNA by snake venom phosphodiesterase (SVPDE). (**B**) RNase H cleavage pattern of the hybrid duplexes. Long and short arrows represent major and minor sites respectively (after 2 h of incubation). Boxes represent the parts of the RNA sequence insensitive towards RNase H cleavage. The percentage of the complementary RNA cleavage by RNase H is summarized in Table 2 (see also Experimental section for details of the protocol).

Table 1 The T_ms (1 μM of each strand) and the thermodynamic parameters of AON–RNA (**26**) hybrids (see Fig. 1 and Experimental section)

AON	T_m/°C	ΔT_m/°C	$-\Delta H°$/kJ mol^{-1}	$-\Delta S$/eu	$-T\Delta S°$	$-\Delta G°_{298}$/kJ mol^{-1}	$-\Delta\Delta G°_{298}$/kJ mol^{-1}
1	44	—	494 ± 32	1.4	429	65	—
2[a]	38	−6	413 ± 35	1.2	360	53	12
3[a]	39	−5	501 ± 28	1.4	442	59	6
4[a]	40	−4	465 ± 15	1.4	408	57	8
5[a]	39	−5	438 ± 40	1.3	381	56	9
6	33	−11	404 ± 5	1.2	357	47	18
7	33	−11	417 ± 13	1.2	372	45	20
8	33	−11	424 ± 17	1.2	375	49	16
9	32	−12	414 ± 5	1.2	369	45	20
10	23	−21	355 ± 26	1.0	322	34	31
11	26	−18	377 ± 25	1.1	339	39	26
12	26	−18	381 ± 25	1.1	342	38	27
13	27	−17	369 ± 22	1.1	330	40	25
14	26	−18	384 ± 15	1.1	345	39	26
16	34	−10	445 ± 15	1.3	393	51	14
17	34	−10	422 ± 12	1.2	375	47	18
18	34	−10	396 ± 12	1.1	348	48	17
19	19	−25	233 ± 14	0.6	202	31	34
20	9	−35	250 ± 7	0.7	229	21	44
24	49	+5	525 ± 8	1.5	450	75	+10
25	34	−10	420 ± 13	1.2	372.7	47	18

[a] Taken from ref. 8*b* for comparison with other double and triple oxetane-modified AONs (see Fig. 1).

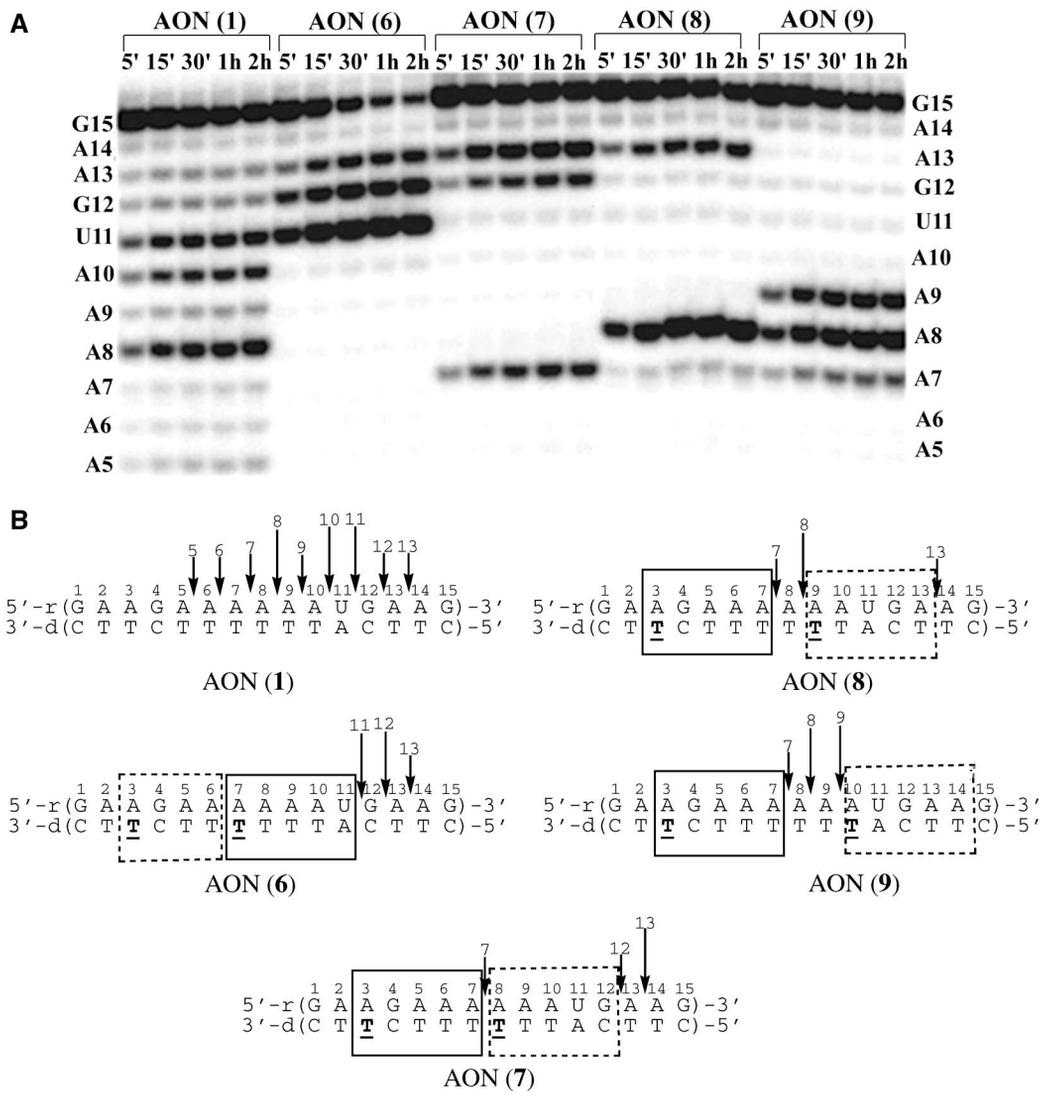

Fig. 3 (**A**) The PAGE analysis of RNase H hydrolysis of the hybrid duplexes, AON (**1**) and AON (**6**)–(**9**)–RNA (**26**). Time after the addition of the enzyme is shown on the top of each gel lane. The length and sequence of 5′-^{32}P-labeled RNAs formed upon enzymatic cleavage are shown on the left and right side of the gel and they were deduced by comparing the migration of products with those oligonucleotides generated by partial digestion of the target RNA by snake venom phosphodiesterase (SVPDE). (**B**) RNase H cleavage pattern of the hybrid duplexes. Long and short arrows represent major and minor sites respectively (after 2 h of incubation). Boxes represent the parts of the RNA sequence insensitive towards RNase H cleavage. The percentage of the complementary RNA cleavage by RNase H is summarized in Table 2 (see also Experimental section for details of the protocol).

Table 2 Extent of hydrolysis of the target RNA (**26**) by RNase H when hybridized to AONs (**1**)–(**25**) after 2 h of incubation with the enzyme (see Experimental section and Figs. 2–7)

AONs	Extent (%) of RNase H cleavage	AONs	Extent (%) of RNase H cleavage
(A) Native		(E) All T modifications	
1	68 ± 3	**15**	0
(B) Single T modifications		(F) Single mismatch	
2	65 ± 5	**16**	66 ± 3
3	68 ± 4	**17**	62 ± 3
4	53 ± 2	**18**	51 ± 4
5	68 ± 2	(G) Triple mismatch	
(C) Double T modifications		**19**	35 ± 2
6	66 ± 2	**20**	0
7	54 ± 3	**21**	0
8	53 ± 2	**22**	0
9	51 ± 3	**23**	0
(D) Triple T modifications		(H) Native with 3′-DPPZ	
10	67 ± 2	**24**	46 ± 6
11	60 ± 5	(I) Triple T with 3′-DPPZ	
12	61 ± 6	**25**	59 ± 4
13	54 ± 4		
14	55 ± 5		

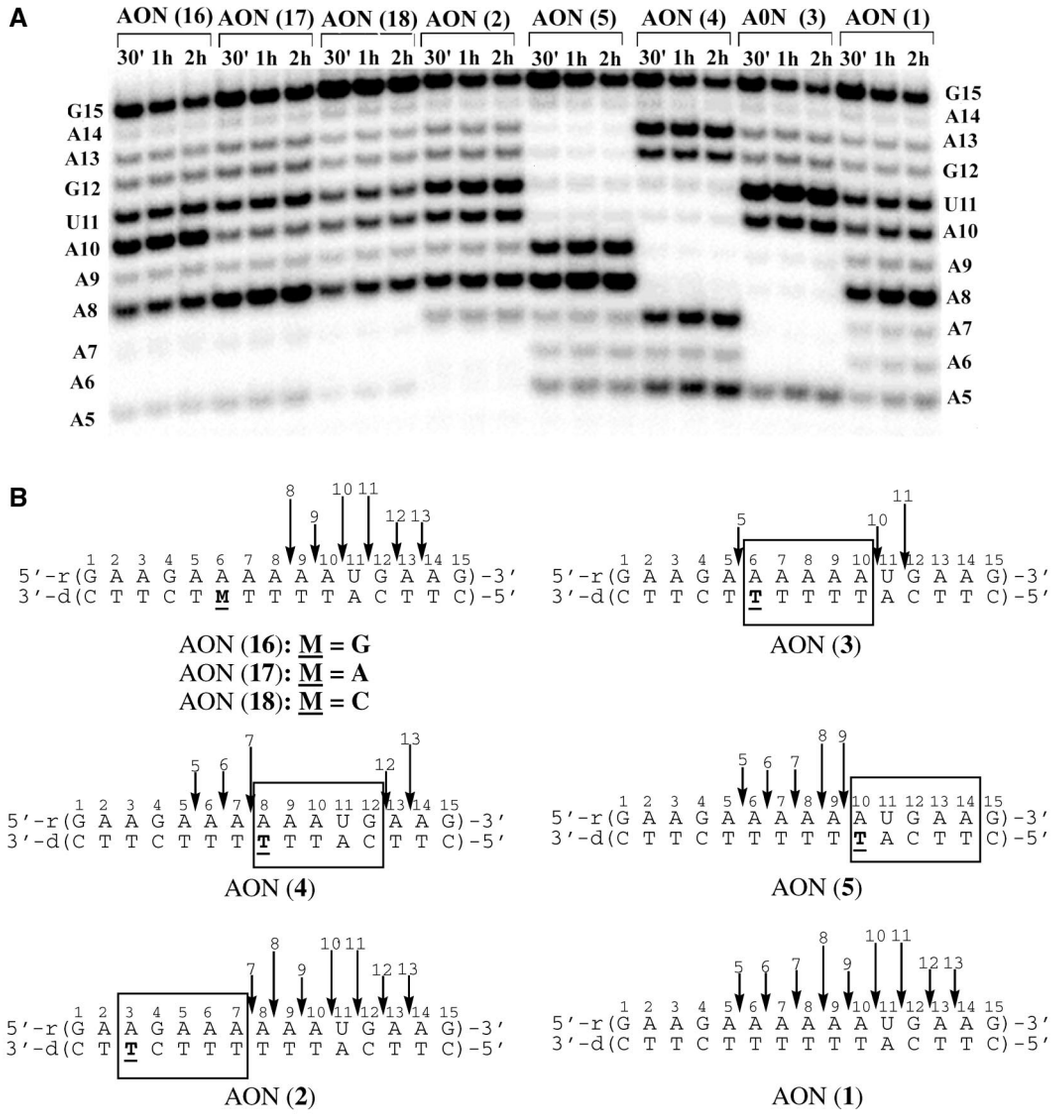

Fig. 4 (**A**) The PAGE analysis of RNase H hydrolysis of the hybrid duplexes, AON (**1**)–(**5**) and (**16**)–(**18**)–RNA (**26**). Time after the addition of the enzyme is shown on the top of each gel lane. The length and sequence of 5′-^{32}P-labeled RNAs formed upon enzymatic cleavage are shown on the left and right side of the gel and they were deduced by comparing the migration of products with those oligonucleotides generated by partial digestion of the target RNA by snake venom phosphodiesterase (SVPDE). (**B**) RNase H cleavage pattern of the hybrid duplexes. Long and short arrows represent major and minor sites respectively (after 2 h of incubation). Boxes represent the parts of the RNA sequence insensitive towards RNase H cleavage. The percentage of the complementary RNA cleavage by RNase H is summarized in Table 2 (see also Experimental section for details of the protocol).

(**10**)–RNA (67 ± 2%) hybrid duplex. In the other three mismatched AONs (**20**)–(**23**), the mismatches are scattered along the whole oligonucleotide chain; these contribute considerably to the structural distortions all along the duplex. This prevents the RNase H promoted cleavage of the target. These mismatch experiments clearly allow us to conclude the following: (i) the triple **T** effect in the AONs (**10**)–(**14**)–RNA (**26**) hybrid duplexes is not a mismatch effect, and (ii) the triple **T** does not interfere with the self-organization of AONs (**10**)–(**14**)–RNA (**26**) hybrid duplexes (which is necessary for the RNase H cleavage) although there is a T_m loss of ~18 °C in the case of three **T** modifications.

(5) Further evidence that distinguishes the **T** effect from the mismatch effect comes from the T_m comparison. When three A mismatches were introduced at the position of three locked **T**s, a dramatic drop in T_m was observed for (**19**)–(**23**) compared to (**10**)–(**14**). For example, in the case of AON (**19**), where mismatches are close to each other, ΔT_m was found to be −25 °C, $\Delta\Delta G°_{298} \approx 34$ kJ mol^{-1} (for the corresponding **T** modified AON (**10**) had T_m of −21 °C, $\Delta\Delta G°_{298} \approx 31$ kJ mol^{-1}), and when the mismatches were scattered, as in AON (**20**), ΔT_m was found to be −35 °C, $\Delta\Delta G°_{298} \approx 44$ kJ mol^{-1} (the corresponding **T** modified AON (**11**)–(**14**) had ΔT_m of −18 °C, $\Delta\Delta G°_{298} \approx 27$ kJ mol^{-1}).

(6) The three **T** modified AONs gave an endonuclease stability (with DNase 1) almost 4-fold better (87% of AON remained after 1 h of incubation, see Fig. 11) compared to the natural counterpart (19% left), but their 3′-exonuclease stability was identical to that of the native AON (**1**) (Fig. 12). The 3′-exonuclease stability was however improved by using three **T** modifications along with the 3′-tethering of the DPPZ moiety, as in AON (**25**), in that 85% of AON (**25**) was intact while the native AON was completely hydrolyzed after 2 h of incubation with SVPDE (note that the endonuclease resistance remained however unchanged). By the same token, RNase H promoted cleavage of AON (**25**)–RNA (**26**) duplex (59 ± 4%) (Fig. 7) remained very comparable to that of the counterpart with the native AON (**1**) (68 ± 3%) and three **T** modified AON (**12**) (61 ± 6%), although a gain of 7 °C of T_m was achieved by this additional 3′-DPPZ modification in **25** compared to **12**. *This again shows that the rise of T_m does not necessarily dictate the RNase H cleavage rate*. This is consistent with what was

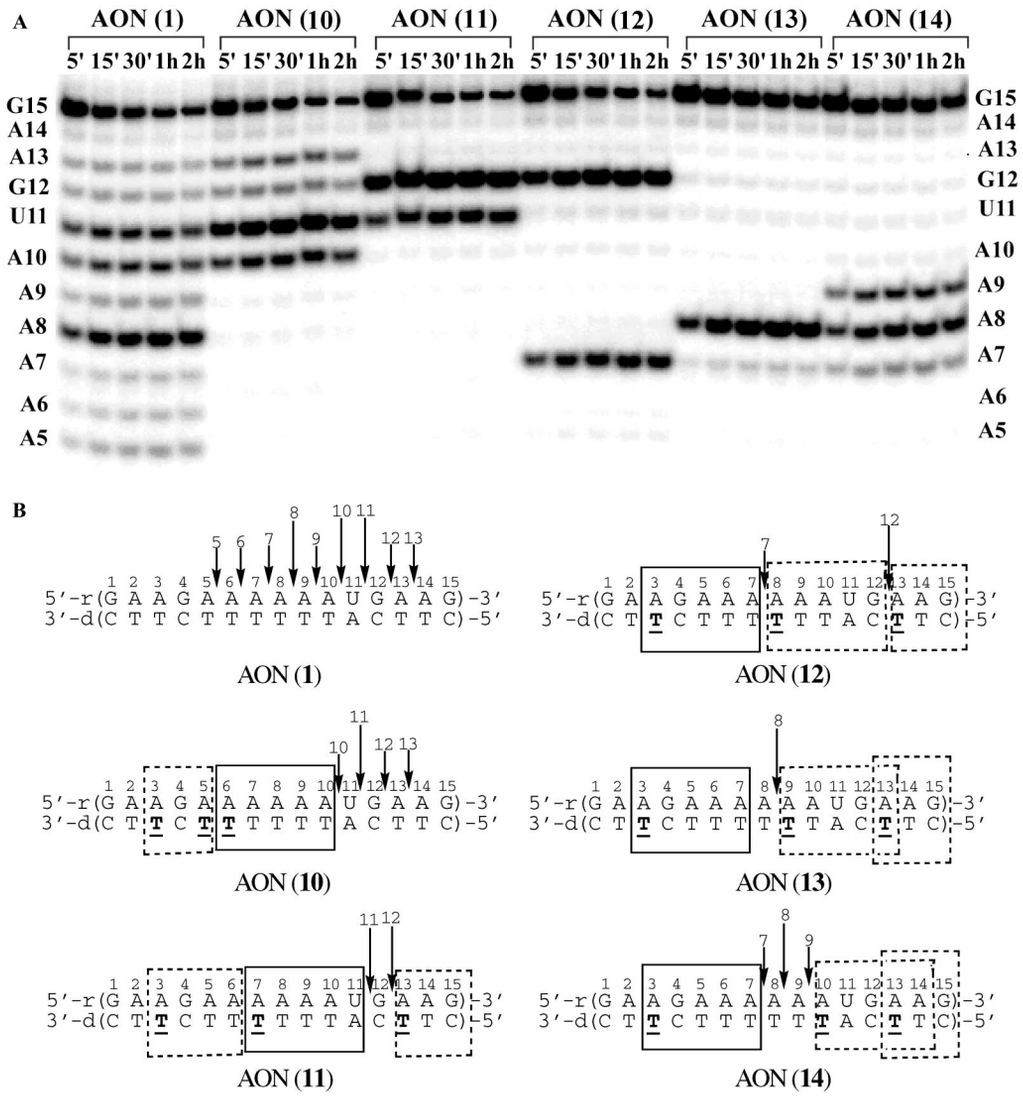

Fig. 5 (**A**) The PAGE analysis of RNase H hydrolysis of the hybrid duplexes, AON (**1**) and (**10**)–(**14**)–RNA (**26**). Time after the addition of the enzyme is shown on the top of each gel lane. The length and sequence of 5′-^{32}P-labeled RNAs formed upon enzymatic cleavage are shown on the left and right side of the gel and they were deduced by comparing the migration of products with those oligonucleotides generated by partial digestion of the target RNA by snake venom phosphodiesterase (SVPDE). (**B**) RNase H cleavage pattern of the hybrid duplexes. Long and short arrows represent major and minor sites respectively (after 2 h of incubation). Boxes represent the parts of the RNA sequence insensitive towards RNase H cleavage. The percentage of the complementary RNA cleavage by RNase H is summarized in Table 2 (see also Experimental section for details of the protocol).

found for some methylphosphonate chimeras[7] and boranophosphates,[11] which had lower T_m values but higher cleavage rates compared to the natural counterpart. However, it should be noted that the presence of the 3′-DPPZ moiety in **25** produces an additional cleavage site at A5 compared to **12** (Fig. 7). This is most probably owing to the stabilization of the terminal G–C hydrogen bonding by the 3′-DPPZ group (observed by NMR[12]) as well as the recognition of the DPPZ by the enzyme,[4b] both of which appear to be important for RNase H recognition, binding and cleavage. Interestingly, amongst all of the **T** modified AONs studied so far, this is the only example where the 5-nucleotide resistance rule in the RNA strand is not obeyed.

(7) The AON (**15**)–RNA (**26**) where all of the Ts were replaced by **T** could not evoke any RNase H promoted cleavage (Fig. 2) because AON (**15**) could not form a hybrid duplex with the target RNA, which was evident from the absence of any UV melting.

(8) The enthalpy of stabilization ($\Delta H°$), as a measure of hydrogen bonding and stacking interactions,[13] can be used to judge the basepairing ability of AONs. AON (**10**) with three **T** modifications had a $\Delta H°$ value of -355 ± 26 kJ mol^{-1}, while the corresponding AON (**19**)–RNA hybrid with three A mismatches has a $\Delta H°$ of only -233 ± 14 kJ mol^{-1}. This large enthalpy difference between mismatched and **T** modified AON–RNA hybrids clearly rules out the possibility of the complete loss of hydrogen bonding in the **T** modified duplexes.

This observation is also supported by the RNase H digestion pattern and the extent of hydrolysis of the mismatched *vis-à-vis* modified duplexes (*vide supra*). Since the magnitude of the enthalpy for the duplex with three **T** modifications lies between those of the native and mismatched duplexes, there is probably a partial loss of basepairing when the AON containing **T** modification forms duplexes with target RNA. Probably, that is the reason why there was no duplex formation detected when ten **T**s were introduced into the AON (as in **15**). It should also be mentioned that the presence of the oxetane moiety of **T** in the minor groove of the duplex might have altered the spine of hydration, which could also contribute to the destabilization of the duplex. Anyway, thorough structural investigations are necessary (some of them are underway in this laboratory) before any conclusion can be drawn on the mechanism.

The RNase H recruiting power of the locked **T** modified AON–RNA hybrids (as in Fig. 1) raises questions on the relation between thermodynamic stability/flexibility of hybrid duplexes and the structure/dynamic *vis-à-vis* recognition, struc-

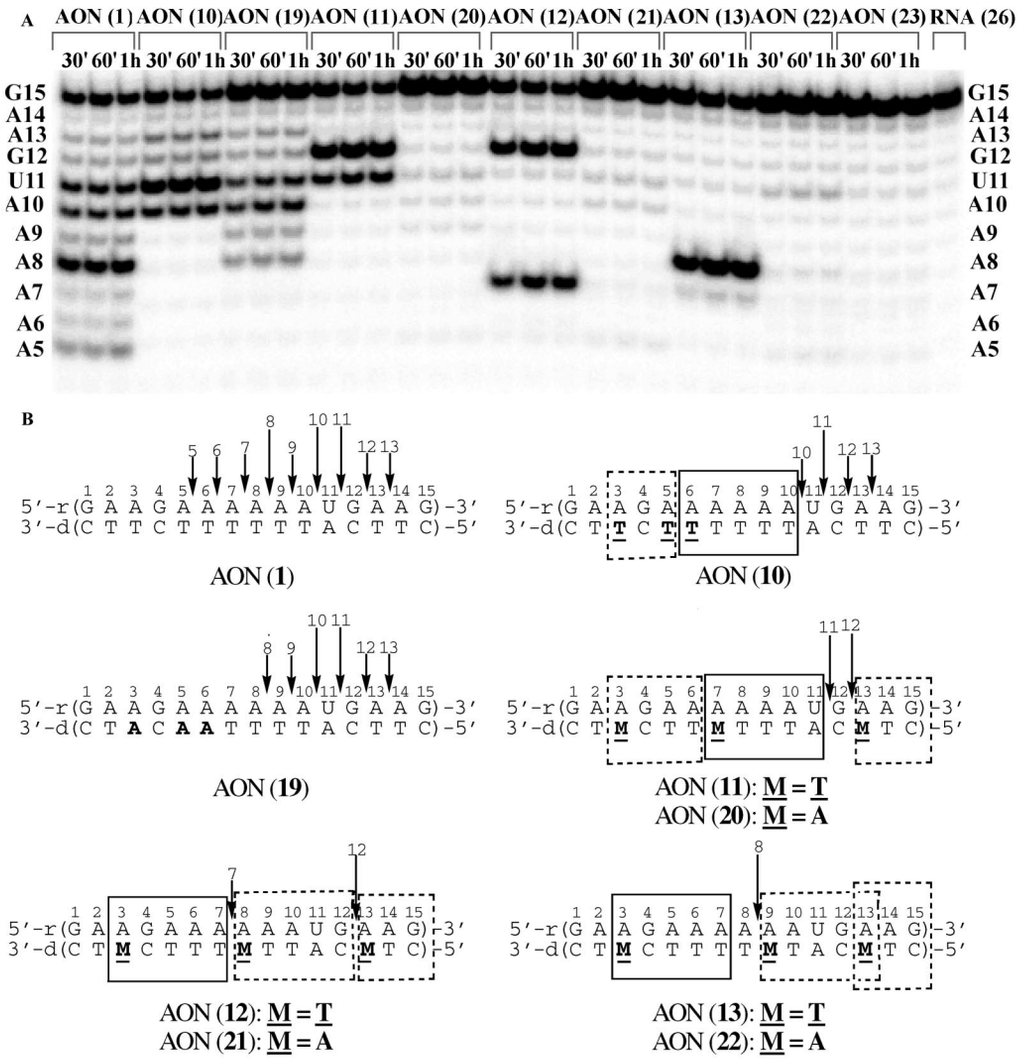

Fig. 6 (**A**) The PAGE analysis of RNase H hydrolysis of the hybrid duplexes, AON (**1**), (**10**)–(**13**) and (**19**)–(**23**)–RNA (**26**). Time after the addition of the enzyme is shown on the top of each gel lane. The length and sequence of 5′-^{32}P-labeled RNAs formed upon enzymatic cleavage are shown on the left and right side of the gel and they were deduced by comparing the migration of products with those oligonucleotides generated by partial digestion of the target RNA by snake venom phosphodiesterase (SVPDE). (**B**) RNase H cleavage pattern of the hybrid duplexes. Long and short arrows represent major and minor sites respectively (after 2 h of incubation). Boxes represent the parts of the RNA sequence insensitive towards RNase H cleavage. The percentage of the complementary RNA cleavage by RNase H is summarized in Table 2 (see also Experimental section for details of the protocol).

tural tolerance and hydrolytic cleavage by the enzyme.[14] It is perhaps important that AON–RNA hybrids should possess a certain degree of structural flexibility, as in our AON–RNA hybrids, in order to undergo certain conformational readjustments necessary for the cleavage reaction[14] upon complexation with RNase H and Mg^{2+} in the minor groove. Those hybrid duplexes which are highly stable have poor conformational flexibility, and are not capable of structurally adjusting themselves upon complexation to the RNase H and Mg^{2+} to form an activated complex to give the cleavage reaction.[14] This may be the reason why RNase H does not hydrolyse those AON–RNA hybrid duplexes which are very stable. Since the RNase H cleavage of the complementary RNA is a slower process than the self-assembly of the AON–RNA hybrid,[4b] a smaller population of the hybrid duplex might actually be adequate to bind to RNase H and drive the complementary RNA cleavage to completion. We expect this to be the case under non-saturation conditions for hybrid duplexes with relatively low T_m as in our oxetane-modified systems, as well as in some methylphosphonate chimeras[7] and boranophosphates.[11]

Conclusions

(1) Introduction of **T** modifications into a 15 mer AON strand in the corresponding AON–RNA heteroduplex resulted in the loss of ~6 °C in T_m/modification.

(2) Irrespective of the loss in T_m, all the single, double and triple **T** modified AON–RNA hybrids were found to be as good a substrate for RNase H as the native hybrid duplex. All **T** modified AON–RNA hybrid was not a substrate to RNase H.

(3) The **T** modified AONs showed improved protection towards endonuclease (DNase 1).The stability towards endonuclease increased with increasing number of **T** modifications. Thus, this is the first example in the literature which shows the introduction of the sugar-constrained nucleotides not only provides endonuclease protection, it also recruits RNase H response in a satisfactory manner.

(4) The loss in thermodynamic stability of the hybrid AON–RNA duplex (as in **12**) was partially compensated (by 7 °C) by the introduction of the DPPZ moiety at the 3′-end of AON (as in **25**), and allowed the complementary RNA strand to retain the full cleaving efficiency by RNase H as that of the native. Noteworthy is the fact that the stability increase of **25** did not enhance its relative RNA cleavage *vis-à-vis* **12**. However, the most important advantage of the 3′-DPPZ introduction is the protection against the 3′-exonuclease, while retaining at the same time the desired endonuclease stability.

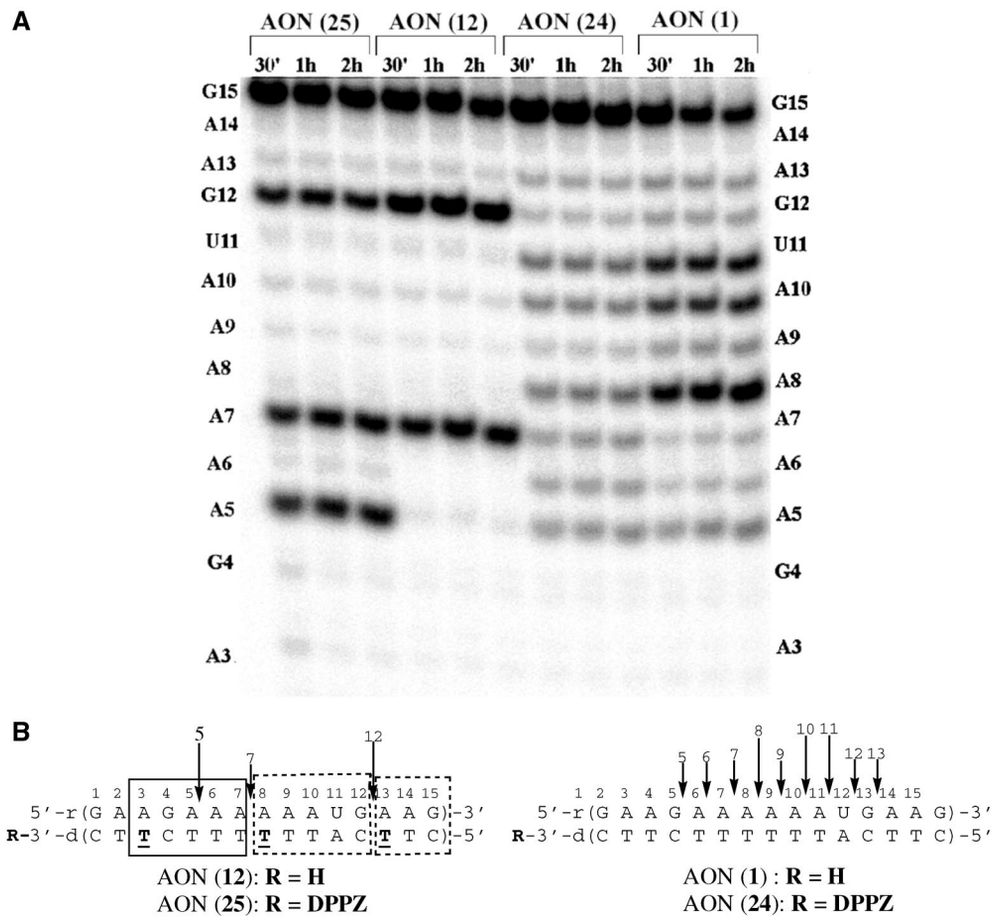

Fig. 7 (**A**) The PAGE analysis of RNase H hydrolysis of the hybrid duplexes, AON (**1**), (**12**), (**24**) and (**25**)–RNA (**26**). Time after the addition of the enzyme is shown on the top of each gel lane. The length and sequence of 5′-^{32}P-labeled RNAs formed upon enzymatic cleavage are shown on the left and right side of the gel and they were deduced by comparing the migration of products with those oligonucleotides generated by partial digestion of the target RNA by snake venom phosphodiesterase (SVPDE). (**B**) RNase H cleavage pattern of the hybrid duplexes. Long and short arrows represent major and minor sites respectively (after 2 h of incubation). Boxes represent the parts of the RNA sequence insensitive towards RNase H cleavage. The percentage of the complementary RNA cleavage by RNase H is summarized in Table 2 (see also Experimental section for details of the protocol).

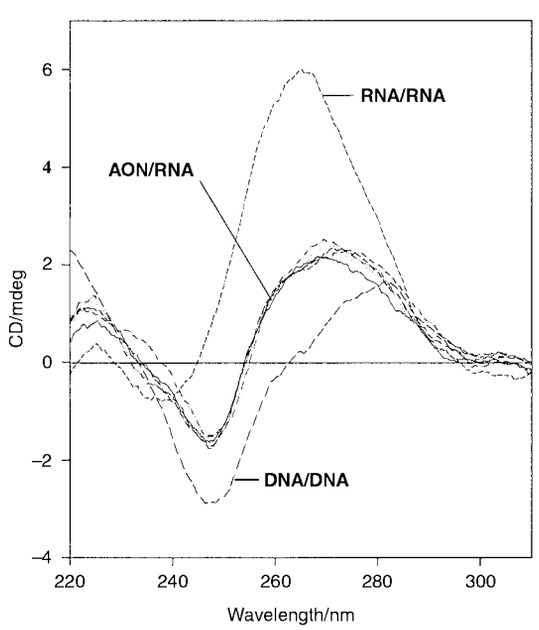

Fig. 8 CD spectra of duplexes formed by AONs (**1**), (**6**)–(**9**) and RNA target (**26**): (——·——) (**1**), (——) (**6**), (——··——) (**7**), (·····) (**8**), (- - -) (**9**). For comparison B type and A type spectra are presented: (—— ——) DNA–DNA duplex formed by AON (**1**) and complementary DNA: 5′-d(GAAGAAAAAATGAAG)-3′, (– – –) RNA–RNA duplex formed by partially self complementary 17 mer RNA: 5′-r(UAACAUGUUUGGACUCU)$_2$.

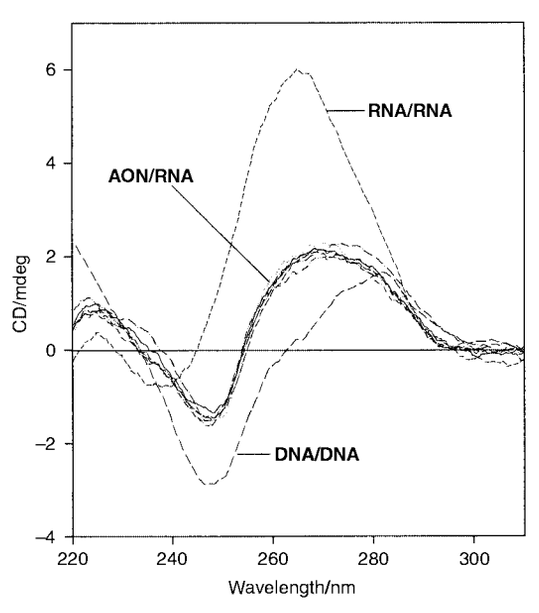

Fig. 9 CD spectra of duplexes formed by AONs (**1**), (**10**)–(**14**) and RNA target (**26**): (——·——) (**1**), (- - -) (**10**), (——) (**11**), (——··——) (**12**), (···+···+···) (**13**), (····) (**14**). For comparison B type and A type spectra are presented: (—— ——) DNA–DNA duplex formed by AON (**1**) and complementary DNA: 5′-d(GAAGAAAAAATGAAG)-3′, (– – –) RNA–RNA duplex formed by partially self complementary 17 mer RNA: 5′-r(UAACAUGUUUGGACUCU)$_2$.

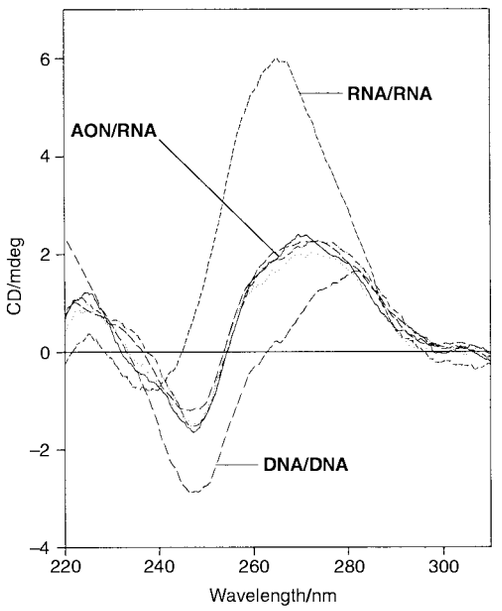

Fig. 10 CD spectra of duplexes formed by AONs (**1**), (**12**), (**24**), (**25**) and RNA target (**26**): (——·——) (**1**), (····) (**12**), (——) (**24**), (——··——) (**25**). For comparison B type and A type spectra are presented: (—— ——) DNA–DNA duplex formed by AON (**1**) and complementary DNA: 5′-d(GAAGAAAAAATGAAG)-3′, (– – –) RNA–RNA duplex formed by partially self-complementary 17 mer RNA: 5′-r(UAACAUGUUUGGACUCU)$_2$.

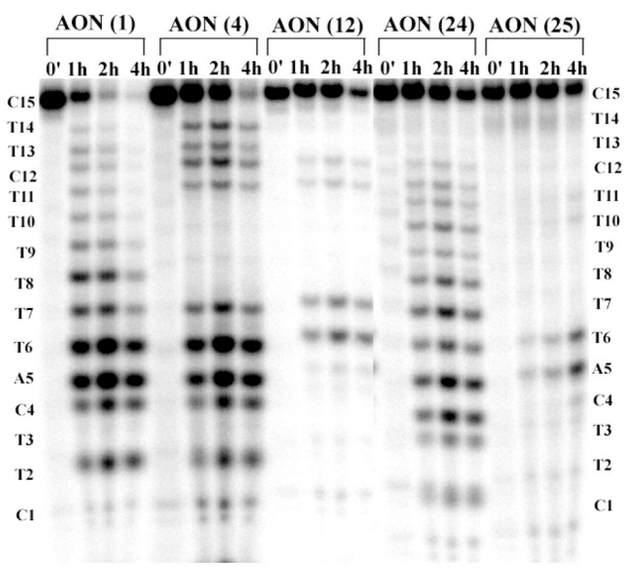

Fig. 11 PAGE analysis of the DNase 1 degradation of AON (**1**), (**4**), (**12**), (**24**) and (**25**). Time in hours after the addition of the enzyme is shown at the top of each gel lane. The percentage of AON left after 1 h of incubation: 19% of AON (**1**), 45% of AON (**4**), 86% of AON (**12**), 51% of AON (**24**) and 87% of AON (**25**).

Materials and methods

Materials

T4 polynucleotide kinase, *E. coli* RNase HI (5 units μL^{-1}) and [γ-^{32}P]ATP were purchased from Amersham Pharmacia Biotech (Sweden), DNase 1 from bovine pancreas and phosphodiesterase I from *Crotalus adamanteus* venom were from Sigma.

Synthesis and purification of oligonucleotides

All oligonucleotides were synthesized using an Applied Biosystems 392 automated DNA/RNA synthesizer. Synthesis, deprotection and purification of all AONs and target RNA were performed as previously described.[8b]

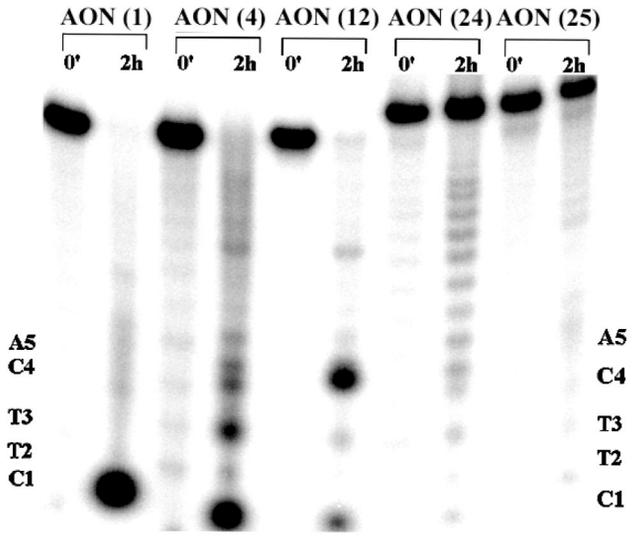

Fig. 12 PAGE analysis of the snake venom phosphodiesterase (SVPDE) degradation of AONs (**1**), (**4**), (**12**), (**24**) and (**25**). Time in hours after the addition of the enzyme is shown at the top of the gel lane. The percentage of AON left after 2 h of incubation with enzyme: 0% of AON (**1**), 0% of AON (**4**), 0% of AON (**12**), 75% of AON (**24**) and 85% of AON (**25**).

UV melting experiments

Determination of the T_ms of the AON–RNA hybrid duplexes was carried out in the same buffer as for RNase H degradation: 57 mM Tris–HCl (pH 7.5), 57 mM KCl, 1 mM $MgCl_2$ and 2 mM DTT. Absorbance was monitored at 260 nm in the temperature range 3 to 70 °C using a Lambda 40 UV spectrophotometer equipped with a Peltier temperature programmer with a heating rate of 1 °C per minute. Prior to the measurements samples (1 : 1 mixture of AON and RNA) were preannealed by heating to 80 °C for 5 min followed by slow cooling to 3 °C and 30 min equilibration at this temperature.

Thermodynamic calculations from the UV experiments

The thermodynamic parameters characterizing the helix-to-coil transition for the DNA–RNA hybrids were obtained from T_m measurements over the concentration range 2 to 10 μM (total strands concentration). Values of $1/T_m$ were plotted *versus* $\ln(C_T/4)$ and $\Delta H°$ and $\Delta S°$ parameters were calculated from the slope and intercept of the fitted line: $1/T_m = (R/\Delta H°)\ln(C_T/S) + \Delta S°/\Delta H°$, where S reflects the sequence symmetry of the self ($S = 1$) or non-self-complementary strands ($S = 4$).

CD experiments

CD spectra were measured on a JASCO J810-A spectropolarimeter from 310 to 220 nm in a thermostatted 0.2 cm path length cuvette. Buffer conditions were the same as for the UV and RNase H experiments: 57 mM Tris–HCl (pH 7.5), 57 mM KCl, 1 mM $MgCl_2$ and 2 mM DTT. A total strand concentration of 2 μM was used in the experiments with AON–RNA hybrids. CD spectra of all the hybrids were measured at 5 °C and each spectrum is an average of 5 experiments from which the CD value for the buffer was subtracted.

^{32}P Labeling of oligonucleotides

The oligoribonucleotides and oligodeoxyribonucleotides were 5′-end labeled with ^{32}P using T4 polynucleotide kinase, [γ-^{32}P] ATP. Labeled AONs and RNA were purified by 20% denaturing PAGE and specific activities were measured using a Beckman LS 3801 counter.

RNase H digestion assays

DNA–RNA hybrids (0.8 μM) consisting of a 1 : 1 mixture of

antisense oligonucleotide and target RNA (specific activity 50000 cpm) were digested with 0.3 U of RNase H in 57 mM Tris–HCl (pH 7.5), 57 mM KCl, 1 mM $MgCl_2$ and 2 mM DTT at 21 °C. Prior to the addition of the enzyme reaction components were preannealed in the reaction buffer by heating at 80 °C for 4 min followed by 1.5 h equilibration at 21 °C. Total reaction volume was 26 μl. Aliquots (7 μl) were taken after 5, 15, 30, 60 and 120 min and reaction was stopped by addition of an equal volume of 20 mM EDTA in 95% formamide. RNA cleavage products were resolved by 20% polyacrylamide denaturing gel electrophoresis and visualized by autoradiography. Quantitation of cleavage products was performed using a Molecular Dynamics PhosphorImager. *The experiments were repeated at least 4 times and average values of the percentage of cleavage are reported here*.

Exonuclease degradation studies

Stability of the AONs towards 3′-exonucleases was tested using snake venom phosphodiesterase from *Crotalus adamanteus*. All reactions were performed at 3 μM DNA concentration (5′-end ^{32}P labeled with specific activity 50000 cpm) in 56 mM Tris–HCl (pH 7.9) and 4.4 mM $MgCl_2$ at 22 °C. An exonuclease concentration of 70 ng μl^{-1} was used for digestion of oligonucleotides (total reaction volume was 16 μl). Aliquots were quenched by addition of the same volume of 20 mM EDTA in 95% formamide. Reaction progress was monitored by 20% 7 M urea PAGE and autoradiography.

Endonuclease degradation studies

Stability of AONs towards endonuclease was tested using DNase 1 from bovine pancreas. Reactions were carried out at 0.9 μM DNA concentration (5′-end ^{32}P labeled with specific activity 50000 cpm) in 100 mM Tris–HCl (pH 7.5) and 10 mM $MgCl_2$ at 37 °C using 30 unit of DNase 1 (total reaction volume was 22 μl). Aliquots were taken at 60, 120, 180 and 240 min and quenched with the same volume of 20 mM EDTA in 95% formamide. They were resolved in 20% polyacrylamide denaturing gel electrophoresis and visualised by autoradiography.

Acknowledgements

We thank the Swedish Natural Science Research Council (NFR) and the Swedish Engineering Research Council (TFR) for generous funding. We also thank Dr E. Zamaratzki for initial association in this work and Mr D. Ossipov for the synthesis of the DPPZ derivatized solid support.

References

1 M. Manoharan, *Biochem. Biophys. Acta*, 1999, **1489**, 117.
2 (*a*) K.-H. Altman, R. Kesselring, E. Francotte and G. Rihs, *Tetrahedron Lett.*, 1994, **35**, 2331; (*b*) M. A. Siddiqui, H. Ford, C. George and V. E. Marquez, *Nucleosides, Nucleotides*, 1996, **15**, 235; (*c*) V. E. Marquez, M. A. Siddiqui, A. Ezzitouni, P. Russ, J. Wang, W. R. Wanger and D. M. Matteucci, *J. Med. Chem.*, 1996, **39**, 3739; (*d*) S. Obika, D. Nanbu, Y. Hari, K. Morio, Y. In, T. Ishida and T. Imanishi, *Tetrahedron Lett.*, 1997, **38**, 8735; (*e*) A. A. Koshkin, S. K. Singh, P. Nielson, P. Rajwanshi, V. K. Kumar, R. Meldgaard and M. J. Wengel, *Tetrahedron*, 1998, **54**, 3607; (*f*) G. Wang, J.-L. Giradet and E. Gunic, *Tetrahedron*, 1999, **55**, 7707; (*g*) J. Wengel, *Acc. Chem. Res.*, 1999, **32**, 301; (*h*) G. Wang, E. Gunic and J.-L. Giradet, *Bioorg. Med. Chem. Lett.*, 1999, **9**, 1147; (*i*) S. Obika, D. Nanbu, Y. Hari, K. Morio, J. Andoh, K. Morio, T. Doi and T. Imanishi, *Tetrahedron Lett.*, 1998, **39**, 5401; (*j*) M. Sekine, O. Kurasawa, K. Shohda, K. Seio and T. Wada, *J. Org. Chem.*, 2000, **65**, 3571; (*k*) K.-H. Altman, R. Imwinkelried, R. Kesselring and G. Rihs, *Tetrahedron Lett.*, 1994, **35**, 7625; (*l*) S. Obika, K. Morio, Y. Hari and T. Imanishi, *Chem. Commun.*, 1999, 2423; (*m*) S. Obika, K. Morio, Y. Hari and T. Imanishi, *Bioorg. Med. Chem. Lett.*, 1999, **9**, 515; (*n*) R. Steffens and C. Leumann, *Helv. Chim. Acta*, 1997, **80**, 2426; (*o*) R. Buff and J. Hunziker, *Bioorg. Med. Chem.*, 1998, 521.
3 (*a*) P. Herdewijn, *Biochem. Biophys. Acta*, 1999, **1489**, 167; (*b*) P. Herdewijn, *Liebigs Ann. Chem.*, 1996, 1337.
4 (*a*) B. F. Baker and B. P. Monia, *Biochem. Biophys. Acta*, 1999, **1489**, 3; (*b*) E. Zamaratski, D. Ossipov, P. I. Pradeepkumar, N. Amirkhanov and J. Chattopadhyaya, *Tetrahedron*, 2001, **57**, 593.
5 (*a*) S. T. Crooke, *Methods Enzymol.*, 2000, **313**, 3; (*b*) S. T. Crooke, *Biochem. Biophys. Acta*, 1999, **1489**, 31.
6 W. F. Lima and S. T. Crooke, *Biochemistry*, 1997, **36**, 390.
7 R. V. Giles and D. M. Tidd, *Anti-Cancer Drug Des.*, 1992, **7**, 37.
8 (*a*) P. I. Pradeepkumar, E. Zamaratski, A. Foldesi and J. Chattopadhyaya, *Tetrahedron Lett.*, 2000, **41**, 8601; (*b*) P. I. Pradeepkumar, E. Zamaratski, A. Foldesi and J. Chattopadhyaya, *J. Chem. Soc., Perkin Trans. 2*, 2001, 402.
9 H. Inoue, Y. Hayase, S. Iwai and E. Ohtsuka, *FEBS Lett.*, 1987, **215**, 327.
10 T. Nishizaki, S. Iwai and H. Nakumara, *Biochemistry*, 1997, **36**, 2577.
11 V. K. Rait and B. R. Shaw, *Nucleic Acid Drug Dev.*, 1999, **9**, 53.
12 T. V. Maltseva, P. Agback, M. N. Repkova, A. G. Venyaminova, E. M. Ivanova, A. Sandstrom and J. Chattopadhyaya, *Nucleic Acid Res.*, 1994, **22**, 5590.
13 M. E. Burkard, D. H. Turner and I. Tinoco, Jr., in *RNA World*, 2nd edn., R. F. Gesteland, T. R. Cech and J. F. Atkins, Eds., Cold Spring Harbor Laboratory Press, Cold Spring Harbor, NY, 1999, pp. 233–264.
14 E. Zamaratski, P. I. Pradeepkumar and J. Chattopadhyaya, *J. Biochem. Biophys. Methods*, 2001, **48**, 189.